




Cite this: *Environ. Sci.: Processes Impacts*, 2019, 21, 1342

## Assessment of fine particles released during paper printing and shredding processes†

Nara Shin,<sup>a</sup> Kalpana Velmurugan,<sup>b</sup> Cathy Su,<sup>a</sup> Alison K. Bauer<sup>b</sup>  
and Candace S. J. Tsai \*<sup>a</sup>

In this study, we investigated the airborne particles released during paper printing and paper shredding processes in an attempt to characterize and differentiate these particles. Particle characteristics were studied with real time instruments (RTIs) to measure concentrations and with samplers to collect particles for subsequent microscopy and cytotoxicity analysis. The particles released by paper shredding were evaluated for cytotoxicity by using *in vitro* human lung epithelial cell models. A substantial amount of particles were released during both the shredding and printing processes. We found that the printing process caused substantial release of particles with sizes of less than 300 nm in the form of metal granules and graphite. These released particles contained various elements including Al, Ca, Cu, Fe, Mg, N, K, P, S and Si. The particles released by the paper shredding processes were primarily nanoparticles and had a peak size between 27.4 nm and 36.5 nm. These paper particles contained elements including Al, Br Ca, Cl, Cr, Cu, Fe, Mg, N, Na, Ni P, S and Si, as determined by scanning electron microscope-energy dispersive X-ray spectroscopy (SEM-EDS) and single-particle inductively coupled plasma-mass spectroscopy (SP-ICP-MS) analysis. Although various metals were identified in the paper particles, these particles did not elicit cytotoxicity to simian virus-transformed bronchial epithelial cells (BEAS2B) and immortalized normal human bronchial epithelial cells (HBE1). However, future studies should investigate other cytotoxicity effects of these paper particles in various types of lung cells to identify potential health effects of the particles.

Received 7th January 2019  
Accepted 11th April 2019

DOI: 10.1039/c9em00015a

rsc.li/espi

### Environmental significance

Shredding and printing equipment are now recognized as a source of indoor air pollution, especially in the home and work environments. Over the past several decades, the use of office equipment has increased, thus raising concerns regarding potential adverse human health outcomes. This study aimed to determine the characteristics of particles from the operation of shredding and printing equipment that generates airborne particulates, as well as to analyze the released particles *via* microscopy and cytotoxicity analysis. This study should facilitate a broad understanding of exposure assessment of the particles released from indoor shredding and printing by consumers, including details regarding particle size and elemental composition, as well as cell viability in those who are exposed.

## Introduction

Many employees work 8 h per day, and some spend more than one-third of the day in various indoor settings such as manufacturing industries, offices, and laboratories in the workplace. However, most workers are not aware of either the indoor air quality or their potential exposure to hazardous

substances in the workplace. Indoor air quality depends on various factors, such as the frequency of contaminant release, the type and amount of particles released from equipment use, the air ventilation exchange rate and the intake air quality.<sup>1–3</sup> Over the past decade, indoor air quality issues have increasingly raised concerns, and some studies have reported potential causes of indoor air quality issues and their consequent health effects.<sup>3–7</sup> With the accelerated development of technology, printers have now become common equipment at home and in the workplace. Karrasch *et al.* have investigated the effects of laser printer device particle release on human subjects in low-level and high-level exposures and have reported 15 symptoms related to laser printer release in 37 subjects.<sup>6</sup> Many factors contribute to particle release, especially from printers; these factors include the temperature, speed of printing, toner components and fuser.<sup>8,9</sup> Toner, a potential major source of

<sup>a</sup>Department of Environmental and Radiological Health Sciences, College of Veterinary Medicine and Biomedical Sciences, Colorado State University, 1681 Campus Delivery, Fort Collins, CO, 80528, USA

<sup>b</sup>Department of Environmental and Occupational Health, Colorado School of Public Health, University of Colorado Anschutz Medical Campus, Aurora, CO, 80045, USA. E-mail: Candace.Tsai@colostate.edu; Fax: +1 970 491 2940; Tel: +1 970 191 1340

† Electronic supplementary information (ESI) available. See DOI: 10.1039/c9em00015a



printer particle release, consists of various components, including thermoplastic polymers and styrene-acrylate copolymers. These substances are fixed onto paper in a process called 'fusing' during printing.<sup>10</sup> This process raised concerns, so toxicological studies have been performed using bronchoalveolar lavage fluids (BALF) cells and alveolar macrophages in mice exposed to toner particles to evaluate the effects. An increase in total BALF cell number and a decrease in body weight have been observed during the recovery phase (9, 28, 56, and 84 days) after exposure in mouse models.<sup>10</sup> Pirela *et al.* have shown that exposure to printer released particles elicits biological responses in human cell lines, such as substantial damage to membrane integrity and increased release of pro-inflammatory cytokines.<sup>11</sup>

Tsai *et al.* have investigated the airborne particles emitted inside the shredder basket during paper shredding.<sup>12</sup> A substantial amount of particles containing various elements such as C, Pt, Si, and Ca, and ranging in size from nanometers to micrometers, were found inside the shredder.

Although the scientific studies shown above have indicated that exposure to printer released particles causes self-reported symptoms and biological responses from animal and human cell lines, the characteristics of the printer released particles, as well as the particles released from paper manipulation have yet to be addressed.<sup>6,10–13</sup> The characteristics of these particles may contain important information to understand the associated respiratory-related symptoms caused by heavy printer and shredder use in an indoor environment.<sup>1,6,7,10–17</sup> The knowledge of the potential biological effects associated with the toxicity of these particles and its concentration levels in the air are necessary, but have not yet attracted the sufficient public attention needed to support further investigation. This research aimed to characterize the particle release from the printing and shredding of plain and printed paper, and to investigate the potential toxicity of the released paper particles by using *in vitro* cytotoxicity assays.

## Materials and methods

The study comprised four parts: (1) evaluation of printer particle release, (2) evaluation of particle release from the shredding of plain and printed paper, (3) microscopy analysis of the released particles and (4) evaluation of the *in vitro* cytotoxicity of paper particles released during shredding.

### Equipment

Direct reading real time instruments (RTIs), including a NanoScan scanning mobility particle sizer (NanoScan SMPS) (model 3910, TSI, Shoreview, MN, USA) and an optical particle sizer (OPS) (model 3330, TSI, Shoreview, MN, USA) were used in this study. The NanoScan SMPS measures particle size ranges of 10–420 nm, as monitored in NanoScan manager software (version 1.0.0.19). The OPS measures a particle size range of 0.3–10  $\mu\text{m}$ , as monitored in aerosol instrument manager software (version 9.0.0.0). Both instruments recorded data with a 1 min response

time; the NanoScan SMPS was operated at a flow rate of 0.9 L min<sup>-1</sup>, and the OPS was operated at a flow rate of 1.0 L min<sup>-1</sup>.

A Tsai diffusion sampler (TDS) was used to collect particles in the respirable and nanometer size ranges.<sup>18</sup> The TDS uses a transmission electron microscopy (TEM) copper grid (400 mesh with SiO<sub>2</sub> film coating, SPI, West Chester, PA, USA) attached to the center of a 25 mm-diameter polycarbonate membrane filter (0.22  $\mu\text{m}$  pore size, Millipore, Billerica, MA, USA) as the sampling substrate to collect particles and it was operated at a flow rate of 0.3 L min<sup>-1</sup>.<sup>18</sup> One polycarbonate filter and one TEM grid were used to sample particles for each experiment.

**(1) Printer particle release test.** Experiments were conducted in a NanoHood (Labconco, Kansas City, MO, USA). The high-efficiency particulate air (HEPA) filtration of the NanoHood was always in operation during the experiments. The atmospheric temperature and relative humidity during each experiment were measured with a VeloCalc air velocity meter (model 9515, TSI, Shoreview, MN, USA); the average relative humidity was approximately 51.3%, and the average temperature was 20–21 °C.

Particle release tests were conducted to assess the release and its constituents related to the toner use (TN420, Brother, Bridgewater, NJ, USA) during paper printing. The printer exhaust fan (D06K-24TU, Nidec Corporation, St. Louis, MO, USA) fixed in a monochrome laser printer (HL-2270DW, Brother, Bridgewater, NJ, USA) had a maximum air flow rate of 0.63 m<sup>3</sup> min<sup>-1</sup>. The same monochrome laser printer, toner, and paper (multipurpose copy paper, 8 $\frac{1}{2}$ "  $\times$  11", #513096, Staples, Framingham, MA, USA) were used for all experiments. Particle release was studied during the printing 1000 sheets of paper and was compared with the release in control experiments, running 1000 blank sheets of paper. To improve measurements, a custom-made hood compartment was attached to the printer exhaust port, as shown in Fig. 1a, to contain the released particles within the hood space for

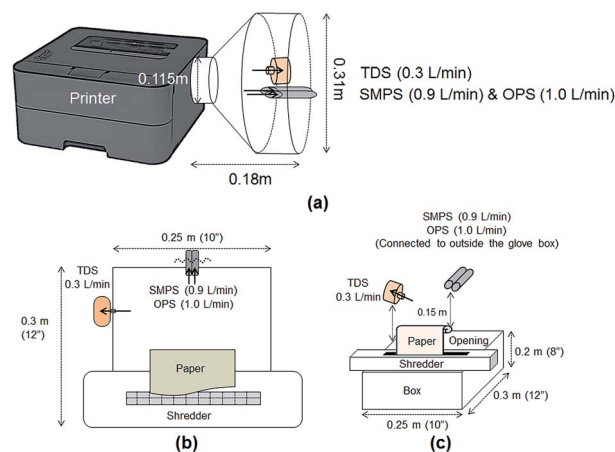


Fig. 1 Illustration of the release test experimental setup. (a) Front view of the printer release experiment setup. (b) Top view of the shredding experiment setup. (c) Three-dimensional view of the shredding experiment setup.



consistent measurement and collection in each experiment. The hood was an approximately 160° angled cone hood with a 0.115 m (4.5 in) inlet diameter, 0.305 m (12 in) outlet diameter and 0.18 m (7 in) duct length. The measurements were taken approximately 0.14 m horizontally from the center of the printer exhaust port, and the average air velocity at this sampling location was approximately 0.3 m s<sup>-1</sup>. The entire surface of the hood was wiped with isopropyl alcohol before and after each experiment.

Tubing 0.45 m in length (Tygon, Saint-Gobin, Malvern, PA, USA) was connected to the RTIs and between the sampling pump and TDS to reach the sampling location at the center of the custom-made hood. The total air flow rate of the RTIs and samplers was approximately 2.205 L min<sup>-1</sup>. The paper was printed with a total of 806 words in 10 point font per sheet with black toner only. The RTI measurements were collected for a 10 min background reading at the beginning of the experiment, an approximately 40–43 min reading during the printing portion of the experiment (including paper refilling and toner replacement time) and a 10 min post-experiment background reading. During the paper refilling and toner replacement, the printer was at rest with the motor stopped. These periods are marked as gray highlighted areas in Fig. 2a–f and are denoted as ‘resting time’ in this study. The printing process was repeated three times, but the duration of resting time varied depending on the condition of the printer, such as the presence of a paper

jam. All trials were performed under the same operating conditions with the same number of papers printed. The variations among repeated experiments were due to the resting time needed to clear paper jams and replace toners.

(2) **Paper particles released from shredding activities.** Shredding was performed in a glove box (Series 100, Terra Universal, Fullerton, CA, USA) equipped with ultra-filtered clean air with the RTIs placed outside the glove box, as shown in Fig. 1b and c. The temperature inside the glove box was 20–22 °C, and the relative humidity was between 8.6% and 15%. The average air velocity blown into the glove box at the filter inlet face, located on the ceiling of the glove box, was 2.7 m s<sup>-1</sup> and the average outlet face velocity was 1.4 m s<sup>-1</sup>. The air velocity range in which samplers were located was less than 0.05 m s<sup>-1</sup>.

The shredder was placed on top of a box (0.25 m × 0.30 m × 0.20 m), and 0.9 m-long tubes were used to connect the RTIs to reach the sampling locations for measurements. Fig. 1b shows the top view of the experiment with the location of each device. Measurements were taken at approximately 15 cm above the center line of the shredder, as shown in Fig. 1c. Each device was located on each side of the box to avoid flow interruption, and the total air flow rate was the same as that in the printer particle release tests (2.205 L min<sup>-1</sup>). The shredding experiments were performed with 40 sheets of (1) printed paper and (2) plain paper. The printed papers were obtained from the printer

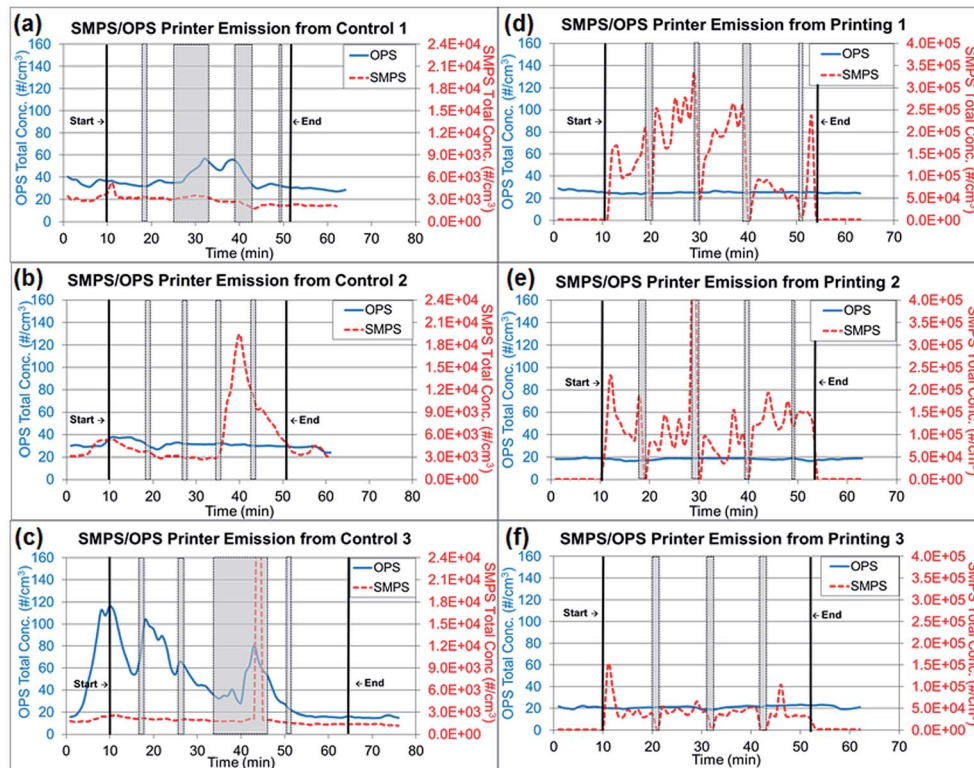


Fig. 2 Real time instrument (RTI) data for particle release tests from running 1000 plain paper sheets and printing 1000 sheets. (a)–(c) Total concentrations from three repeated experiments of running 1000 sheets each, as measured by RTIs. (d)–(f) Total concentrations from three repeated experiments printing 1000 sheets each, as measured by RTIs. Note: Gray highlighted areas represent ‘resting time’ in Fig. 2, which the printer was at rest with the motor stopped for paper refilling and toner replacement.



particle release test and shredded at 30 s intervals for this evaluation. Each shredding experiment was repeated three times. The RTI data were exported into Excel and analyzed for particle number concentration and size distribution. The glove box was wiped clean with de-ionized water before and after each experiment, and the shredder was also wiped with isopropyl alcohol to remove any contamination before and after each experiment. All data were summarized to compare the released particle concentration and size during printing and shredding activities in the experiments.

**(3) Microscopy analysis.** After each experiment, the particles collected on TDS polycarbonate filters and copper grids were analyzed through electron microscopy. Small pieces of polycarbonate filters were coated with 10–15 nm gold and analyzed using scanning electron microscopy (SEM) (JSM-6500F, JOEL, Peabody, MA, USA) and energy dispersive spectroscopy (EDS) (model 51-XXM1015, Concord, MA, USA) at 15 kV. The grids were analyzed using TEM (JEM-2100F, JOEL, Peabody, MA, USA) and EDS (model 51-XXM1058, Concord, MA, USA) at 200 kV. These microscopy analyses were necessary for substances in micrometer to nanometer size range, to understand the morphological characteristics, sizes, and elemental compositions of the studied particles. The analyzed results will allow for identification of typical particles and their constituents which might be exposure risks for humans.

**(4) *In vitro* cytotoxicity assays of paper particles released by shredding activities.** This analysis has been widely used as an indicator of potential biological toxic effects by measuring the viability of cells after exposure to studied particles.

*Generation and collection of paper particles for cytotoxicity assays.* The same shredding method as in (2) paper particles released by shredding activities was used with slight modifications to collect airborne paper particles for cytotoxicity evaluation. A total of 200 sheets, printed in black, with one sheet fed every 30 s, were shredded into a 44 gallon bag placed underneath the shredder, and paper particles inside the bag were collected. The NIOSH manual of analytical methods (NMAM) 0500 method was slightly modified and used to collect particles in 37 mm cassettes with a polycarbonate filter at a flow rate of 1 L min<sup>-1</sup>, instead of a PVC filter. The cassettes were located inside the bag. After shredding, the bag filled with shredded paper was shaken for 2 h for additional particle collection. The average total mass concentrations calculated based on the collected paper dust mass and sampling air volume were  $1.35 \times 10^{-4}$  and  $2.08 \times 10^{-4}$  mg mL<sup>-1</sup> for black and plain paper respectively.

*Preparation for cytotoxicity assays.* The particles collected through the NIOSH NMAM 0500 method were weighed to obtain the mass, and the particles were then suspended in Dulbecco's modified Eagle's medium (DMEM) at a concentration of 10.77 mg mL<sup>-1</sup>, which was the highest concentration (100%) exposed to cells in this experiment. The dose was determined to model the extreme scenarios for cell viability response on biomarkers caused by the exposure. The highest dose (100%) used was approximately 80 000 to 50 000 times higher than the average total mass concentration of paper particles collected using NMAM 0500 method. Several dilutions

(e.g., 100%, 50%, and 25%) of particle suspended media samples were prepared for variations on cell treatment. The prepared particle suspensions in media were further sonicated with a sonic dismembrator (model 100, Fisher Scientific, Hampton, NH, USA) for 20 min in an ice bath.

Cytotoxicity assays used the following human bronchial epithelial cell line models: simian virus-transformed bronchial epithelial cells (BEAS2B, CRL-9609, ATCC, Manassas, VA, USA) and immortalized normal human bronchial epithelial cells (HBE1, a kind gift from Dr Reen Wu's laboratory, University of California, Davis, CA, USA) for treatments of 24–48 h. BEAS2B cells were isolated from normal human bronchial epithelium obtained from autopsies collected from individuals without cancer,<sup>19–24</sup> and HBE1 cells were obtained from a 60 year-old female donor with idiopathic pulmonary fibrosis.<sup>25</sup> Thus, both cell lines are non-transformed.

BEAS2B cells were cultured in DMEM (11885-084, Thermo Fisher Scientific, Waltham, MA, USA) with 10% fetal bovine serum and 1% penicillin/streptomycin (97062-806, VWR, Radnor, PA, USA). HBE1 cells were cultured in DMEM/F12 (D6434, Sigma-Aldrich, St. Louis, MO, USA) with supplements including 2.5 mM L-glutamine (G7513, Sigma-Aldrich), 2.5 µg mL<sup>-1</sup> plasminogen (ant-mpt, InvivoGen, San Diego, CA, USA), 1.5 mg mL<sup>-1</sup> bovine hypothalamus extract (C-30180, BioMedica, PromoCell, USA), 4 µg mL<sup>-1</sup> insulin (#I6643, Sigma-Aldrich), 5 µg mL<sup>-1</sup> transferrin (#T8158, Sigma-Aldrich, St. Louis, MO, USA), 10 ng mL<sup>-1</sup> EGF (#E9644, Sigma-Aldrich), 0.1 µM dexamethasone (D4902, Sigma-Aldrich) and 20 ng mL<sup>-1</sup> cholera toxin (C8052, Sigma-Aldrich). Both cell lines were incubated in a humidified incubator at 37 °C with 5% CO<sub>2</sub>.

*In vitro cytotoxicity assays.* HBE1 and BEAS2B cells were grown to confluence in 96 well plates (15705-066, VWR, Radnor, PA, USA) before paper particle exposure. Serum deprivation was then initiated 24 h before paper particle treatment for the BEAS2B cells and was followed by treatment with two types of paper particles (plain and printed) for 24–48 h. CellTiter 96 Aqueous One Solution Cell Viability assays (MTS assay, Promega, Madison, WI, USA) were then performed to detect cytotoxicity according to the manufacturer's protocol. HBE1 cells were treated with the particles in their medium which were serum-free, similarly to the cells in BEAS2B medium, and cytotoxicity was tested 24–48 h after treatment.

Plates were read at 490 nm with a microplate reader (Infinite 200 PRO NanoQuant Microplate Reader, Tecan, Morrisville, NC, USA). Each concentration was assessed in three replicates per experiment, and the experiments were repeated three times. The cell viability results of three replicates were calculated to determine the standard error of the mean and were standardized by calculating the percentage change relative to control (set at 100%) for each plate.

*Statistical analysis.* Statistical analysis was conducted with the SPSS statistical analysis software package (version 1.0.0.1126, IBM, Armonk, NY, USA). The cell viabilities of two cell lines (BEAS2B and HBE1) treated with various concentrations of paper particles were assessed and evaluated for statistical significance with one-way analysis of variance. At a 95%



confidence level,  $p$ -values < 0.05 were considered statistically significant.

(5) **SP-ICP-MS analysis.** A portion of particle-containing media prepared for cell exposure was analyzed for elemental composition using single particle inductive coupled plasma-mass spectrometry (SP-ICP-MS) with a NexION 350D mass spectrometer (PerkinElmer, Bradford, CT, USA) connected to a self-aspirating nebulizer (PFA-ST nebulizer) (Elemental scientific, Omaha, NE, USA) and a Peltier (PC3x, Elemental Scientific, Omaha, NE, USA) controlled quartz cyclonic spray chamber (Elemental Scientific, Omaha, NE, USA) set at 2 °C. Samples were centrifuged to remove agglomerates and were diluted 100 times with 2% HNO<sub>3</sub>. Samples were introduced with auto-dilution equipment (prepFAST SC-2 autosampler) (Elemental Scientific, Omaha, NE, USA). Before analysis, the nebulizer gas flow and quadrupole ion deflector were optimized for maximum indium signal intensity. A daily performance check was also performed to ensure that the instrument was operating properly and that a CeO<sup>+</sup> to Ce ratio less than 0.025 and a Ce<sup>++</sup> to Ce ratio less than 0.030 were obtained. After suspending the particles in the media, the liquid suspension was injected into the SP-ICP-MS; the detection showed the sizes and elements of nanoparticles. This test was repeated three times. The differences in elemental composition were compared to the blank medium and analyzed with Syngistix's software (PerkinElmer, Bradford, CT, USA).

## Results & discussion

### Printer particle release tests

The measured particle concentrations obtained from RTIs were analyzed and are presented in two types of graphs showing (1) the total particle number concentration changes throughout the entire experiment and (2) the size-fractionated particle number concentration.

The total concentration of each experiment is presented separately in Fig. 2a–c for running 1000 sheets (control) and in Fig. 2d–g for printing 1000 sheets due to the inconsistent resting periods. The experimental periods (pre-experiment, during printing, during resting time and post-experiment) were noted. The average total concentrations and standard deviations throughout the experimental periods were calculated and presented in Table 1. Concentration changes during

printing were calculated in this section by subtracting the pre-experiment concentration, and the background concentration, to adjust the particle concentrations from the environment in the laboratory room. During the printing periods for printing 1000 sheets, the total net concentration of particles smaller than 420 nm (NanoScan SMPS data) increased by approximately 98 600 particles per cm<sup>3</sup> from 1400 particles per cm<sup>3</sup> to 100 000 particles per cm<sup>3</sup>. However, the net increase of running 1000 sheets was approximately 500 particles per cm<sup>3</sup> from 3100 particles per cm<sup>3</sup> to 3600 particles per cm<sup>3</sup>, thus indicating a 200-fold difference between printing and running 1000 sheets. The laboratory where this experiment was performed has the average background concentration of 7000 particles per cm<sup>3</sup> for particle size less than 420 nm and 7 particles per cm<sup>3</sup> for particle size range from 0.3 to 10 μm. The particles released during printing 1000 sheets had 14 and 7 times higher average concentrations than the laboratory background, in particle sizes less than 420 nm and in a range of 3–10 μm respectively. Printing 1000 sheets resulted in a substantial increase in concentration, as also seen through the comparison to the resting time values indicated in gray highlights in Fig. 2d–g. This increase caused by printing paper was apparent on sub-micrometer sized particles measured by NanoScan SMPS but not on larger particles measured by OPS. Currently, there are no health guidelines or standards for particulate number concentrations in the U.S. However, the contribution of high number particle concentration by printing processes to the indoor environments may become a concern.

In the control experiments presented in Fig. 3a and b, the dominant particle size generated from running 1000 sheets peaked at 27 nm, as determined through NanoScan SMPS, and the average concentration was approximately 6000 particles per cm<sup>3</sup> during the experiment. Although this corresponding mode size had a relatively higher concentration than the pre- and post-experiment concentrations, the mode peaked at 27 nm throughout the entire experiment. As discussed previously, when the toner was used for printing of 1000 sheets, the mode size appeared to be smaller (15 nm), with a concentration of approximately 300 000 particles per cm<sup>3</sup>. Thus, the printing process generated substantially more particles with smaller sizes within 10–420 nm than were generated by running the printer. The amount of released particles with larger than sub-

Table 1 Average total concentrations from printer particle release tests, as measured by NanoScan SMPS and OPS<sup>a</sup>

Average total concentration and standard deviation of printer particle release tests (particles per cm<sup>3</sup>)

|                 | OPS             |            | SMPS            |                    |
|-----------------|-----------------|------------|-----------------|--------------------|
|                 | Plain (control) | Printing   | Plain (control) | Printing           |
| Pre-experiment  | 43 (±14)        | 22 (±0.41) | 3100 (±510)     | 1400 (±60)         |
| During printing | 41 (±10)        | 22 (±0.61) | 3600 (±1500)    | 100 000 (±24 000)  |
| Resting time    | 44 (±17)        | 21 (±3)    | 4200 (±8200)    | 110 000 (±160 000) |
| Post-experiment | 24 (±1)         | 21 (±0.41) | 2400 (±184)     | 1800 (±153)        |

<sup>a</sup> Standard deviations are presented in parentheses. During printing, the concentration difference between running and printing 1000 sheets, as determined by NanoScan SMPS, was 98 100 particles per cm<sup>3</sup>.



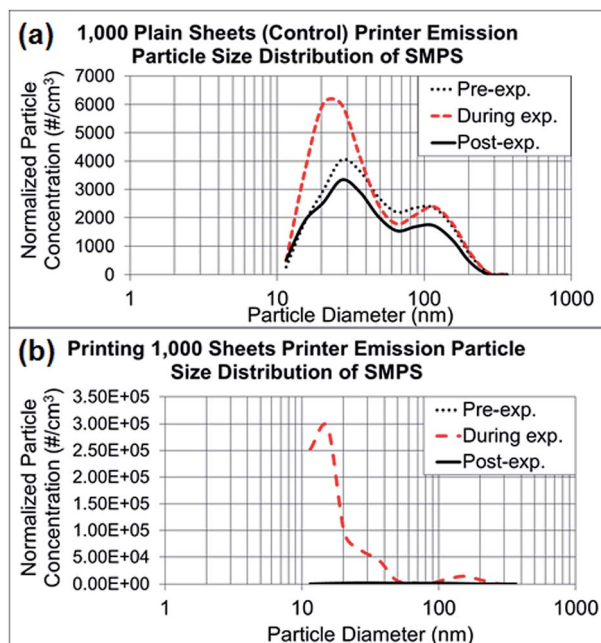


Fig. 3 NanoScan SMPS data of released particle size distribution. (a) Average particle size distributions of three repeated experiments running 1000 sheets each, as represented in Fig. 2a–c. (b) Average particle size distributions of three repeated experiments printing 1000 sheets each, as represented in Fig. 2d–f.

micrometer diameters, as measured by OPS (0.3–10  $\mu\text{m}$ ), did not differ between printing and the control process of running the printer, as presented in ESI Fig. S1a and b.† The OPS mode sizes were 337 nm for both experiments, with a concentration range of 150–350 particles per  $\text{cm}^3$ .

### Morphology and elemental composition analysis of printer release

The printer released particles collected through TDS were in various shapes and sizes. The typical shapes of the particles were granular, irregular and layered. These particles were consistently found through microscopy analysis of samples collected during printing (Fig. 4a–d, 5a and ESI S2a–ff). The sizes of the particles observed under TEM and SEM were in the sub-micrometer range, which corresponded to the RTI measurements of 1  $\mu\text{m}$  or less.

Fig. 4a–d shows the results of granular and irregular shaped particles in TEM analysis and Fig. 4e shows the elemental composition of the particles in EDS analysis. For these particular particles, each granule ranged in size between 1 and 10 nm, and the major elemental composition comprised C, Cu, P, and S. Regardless of whether copper grids were used, Cu was found to account for a major portion of the particle composition. The blank copper grid in EDS analysis showed a 1 : 5 ratio between the  $L\alpha$ -shell and  $K\alpha$ -shell, whereas the copper-containing granular particles displayed a stronger peak ratio between the  $L\alpha$ -shell and  $K\alpha$ -shell (1 : 3 ratio or higher; Fig. 4e), compared with the other types of particles (Fig. S3†).

Another typical observed particle was irregular and layered (Fig. 5a). To identify the characteristics of this type of particle, we used TEM line profile analysis to measure the distance between layers. The interlayer space measurement of the particle was 0.34 nm, a typical carbon bond length. This structural property is commonly identified as graphite, a multi-layer form of carbon, through the established analysis method.<sup>26</sup>

Other than the granular and layered particles, the irregular shaped particles observed under TEM were also analyzed with

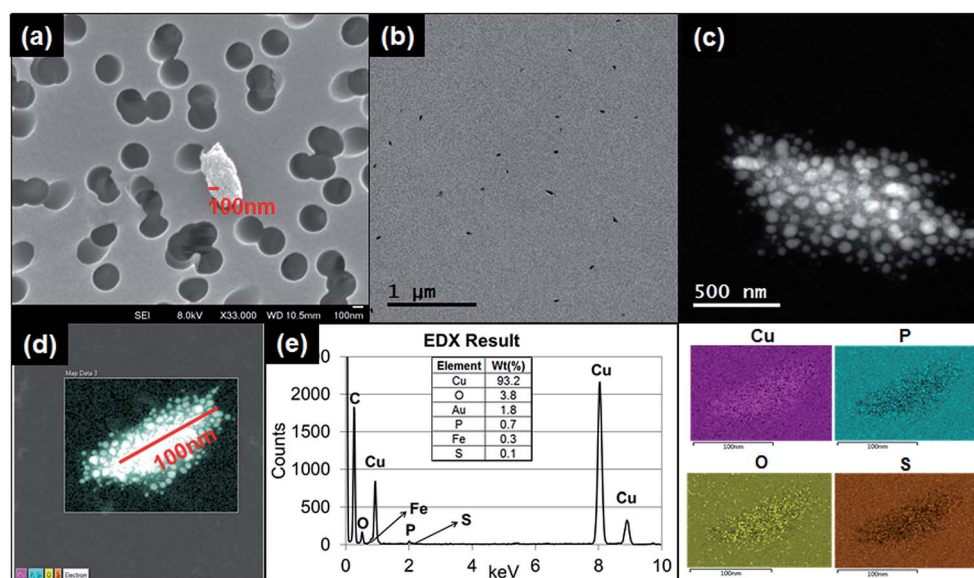


Fig. 4 Microscopy analysis (SEM/TEM/EDS) of printer released particles. (a) SEM image of printer released particles on a TDS polycarbonate filter. (b) TEM image showing collected printer released particles on a TDS copper grid at low magnification. (c) TDS TEM image of printer released particles, with many attached granular particles, at high magnification. (d) TEM-EDS image of analyzed particles with attached granules, as observed through TDS. (e) EDS quantitative analysis of the image in (d) and qualitative analysis indicated by color. Note: Gold (Au) was used as a coating, which was excluded in this analysis.



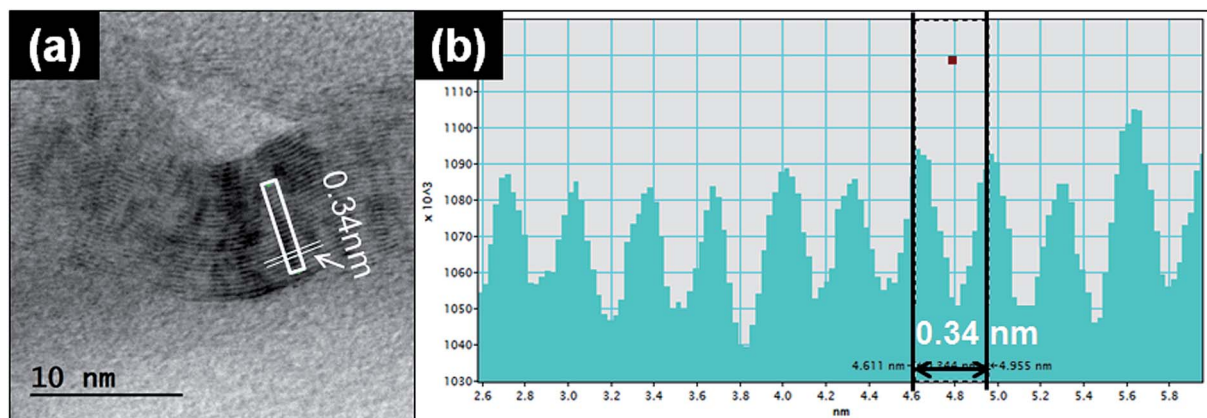


Fig. 5 Graphene TEM lattice analysis. (a) Representative TEM image of graphene particles released from the printer. (b) The intensity line profiles of the selected area from (a).

EDS. The EDS results showed various types of metals from the particles released from both running and printing 1000 sheets. As described in ESI, Fig. S3a† shows irregular shape particles collected by using TDS and analysis through EDS. The peaks in ESI Fig. S3b† show various elements and intensities for each element, including Al, Ca, C, Cu, Fe, K, Mg, N, O, S and Si. The distribution map of each element in the particle is presented in ESI Fig. S3c.†

On the basis of our findings, multiple factors can contribute to the constituents of released particles from printing, such as metal-containing parts inside the printer and the heat generated during printing. The high level of nanoparticle release from a printer can cause respiratory problems and indoor air quality issues in similar environments, such as commercial printing rooms or any locations where printers are in use. As also stated in the NIOSH Pocket Guide to Chemical Hazards, copper may be associated with adverse health effects, such as acceleration of mutation in respiratory tract, skin, liver and kidney cells. Different printers may emit particles with different characteristics and airborne concentrations.

### Paper particles released from shredding activities

The particle concentrations measured from shredding activities were compared among the pre-experimental background, the shredding process and the post-experimental background, and the changes in particle concentration and size distribution were observed (Fig. 6a–c). As presented in Fig. 6a, the paper particle concentration in the 10–420 nm size range (NanoScan SMPS) increased at the beginning of the shredding, and the concentration in the 0.3–10  $\mu\text{m}$  size range (OPS) increased at the end of the shredding experiment. Table S2† summarizes the average concentrations of various particle sizes on both instruments by the first- and second-half (10 min) of shredding time (20 min). There was no indication of a mode size change between the first- and second-half of shredding for OPS measurements. The mode size on OPS was determined to be the same as 337 nm on both the first- and second-half of the shredding period, and as expected the

overall concentrations of all sizes on second-half of shredding period were higher than the first half. The mode size of NanoScan SMPS measurements varied from 20.5 to 36.5 nm

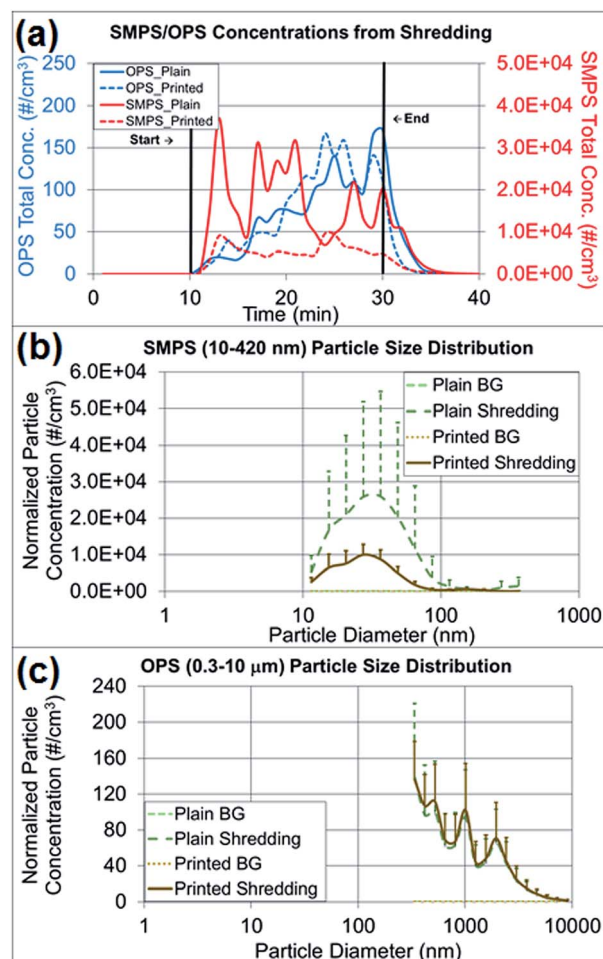


Fig. 6 RTI [OPS (0.3–10  $\mu\text{m}$ ) and NanoScan SMPS (10–420 nm)] data for shredding 40 sheets of plain and printed paper. (a) Area total particle concentration, as measured by RTIs. (b) Paper particle size distribution with standard deviations, as determined by NanoScan SMPS. (c) Paper particle size distribution with standard deviations, as determined by OPS.



and the concentrations did not give a clear indication of concentration increase as seen on OPS measurements. The released paper particles had similar average concentrations of 77–82 particles per cm<sup>3</sup>, on the basis of OPS measurements, regardless of whether plain (control) or printed paper was shredded. However, Table 2, the findings regarding released particles less than 420 nm (NanoScan SMPS) showed that shredding printed paper released three times fewer particles than shredding plain paper. This result was notable in terms of the size distributions and upper standard deviations (Fig. 6b and c). The mode size of the released printed paper particles was 27 nm with a concentration of 10 000 particles per cm<sup>3</sup>, whereas plain paper had a mode size of 37 nm with a concentration of 26 000 particles per cm<sup>3</sup>, a value 2.6 times greater. The high variations of standard deviations (Fig. 6b) are due to the loosely structured plain paper that was not pressed with the toner through the heating process. More small particles were released from plain paper than printed paper due to the structural alteration, as confirmed by the TEM and SEM analyses.

### Analysis of paper surface and elemental composition

To determine the structures of printed paper and plain paper, the surfaces of paper pieces and elemental composition analysis were conducted by using SEM and EDS (Fig. 7a and c) and TEM (ESI Fig. S4†). The surface of the plain paper (Fig. 7a) showed entangled fibers with nano- to micro-meter sized particle agglomerates. The surface of the printed paper (Fig. 7c) had a melted appearance similar to basalt, possibly as a result of the heat pressing during printing with the toner. The composition analysis showed that the printed paper contained Al, Ca, Cl, S and Si (Fig. 7d) and Na, Mg, and P elements were found from both the printed paper and plain paper (Fig. 7b).

### Cytotoxicity effects of released paper particles and elemental composition analysis

In the cytotoxicity study, two human lung cell lines (BEAS2B and HBE1) were treated with paper particles, and the cytotoxicity responses of the cells to the particles were measured (Fig. 8a and b). The cytotoxicity varied substantially and yielded inconsistent results according to statistical analysis ( $p$ -value > 0.05, determined at 95% confidence level, for exposed concentration levels in all types of experiments). For the treated BEAS2B cells, the

cytotoxicity results after exposure to various concentrations did not show significance among different concentrations of paper dust treatment for both plain paper particles ( $p$ -value of 0.866) and printed paper particles ( $p$ -value of 0.603). Similarly, for the treated HBE1 cells, the cytotoxicity responses after exposure to plain paper particles ( $p$ -value of 0.324) and printed paper particles ( $p$ -value of 0.732) at various concentrations did not show significance. In summary, treatment with all concentrations in both cell lines did not yield significant changes in cell viability and appear to increase cell number; thus, there is no evidence that the various levels of paper particle concentrations to which the BEAS2B and HBE1 cells were exposed had significant toxicity effects in terms of cellular response.

Investigating the effect of paper particle exposure on human lung cells is important because of the exposure possibilities to humans in various indoor environments. Although the cytotoxicity results of paper particle exposure showed inconsistency across various concentrations, and no significant differences were observed, this result may not represent the response from human exposure. The cytotoxicity response in humans may differ depending on the particle size, an individual's physical and medical status and susceptibility to the constituents in the paper particles. For example, individuals with asthma may be more susceptible to these particles due to potential co-exposure effects,<sup>27,28</sup> the focus of future studies. In addition, many toxicants are not cytotoxic yet still exert biological effects in the human body; for example, some polycyclic aromatic hydrocarbons can lead to inflammatory mediator production at non-toxic doses in lung epithelial cells.<sup>29</sup> Regardless of the uncertainty of cytotoxicity, the nanometer-sized particles released by the shredding process are still of concern because of their deposition in the alveolar region after inhalation and their potential to enter the bloodstream.

Additionally, the medium alone and the particle suspended medium used for cell treatment were analyzed with SP-ICP-MS to identify the potential elements affecting cytotoxicity. Fig. 9a and b show the average intensity of each element (as the average relative intensity difference relative to blank media from three replicates with standard errors). The original SP-ICP-MS measurement report is presented in ESI Table S1.† The elements Br, Ca, Fe and P were identified from both plain and printed paper, and Al, Cu, and Ni were additionally found from only plain paper. A comparison of SP-ICP-MS and EDS analysis indicated that the elements Al, Ca, and P were commonly

**Table 2** Average total concentration from shredding experiments, as measured by NanoScan SMPS and OPS. Standard deviations are presented in parentheses<sup>a</sup>

|                  | OPS             |                | NanoScan SMPS   |              |
|------------------|-----------------|----------------|-----------------|--------------|
|                  | Plain (control) | Printed        | Plain (control) | Printed      |
| Pre-experiment   | 0.011 (±0.0062) | 0.034 (±0.089) | 5.4 (±3.1)      | 1.3 (±0.75)  |
| During shredding | 77 (±49)        | 82 (±51)       | 17 000 (±9400)  | 5600 (±2200) |
| Post-experiment  | 17 (±29)        | 6.1 (±13)      | 3200 (±4500)    | 710 (±1000)  |

<sup>a</sup> Standard deviations are presented in parentheses.





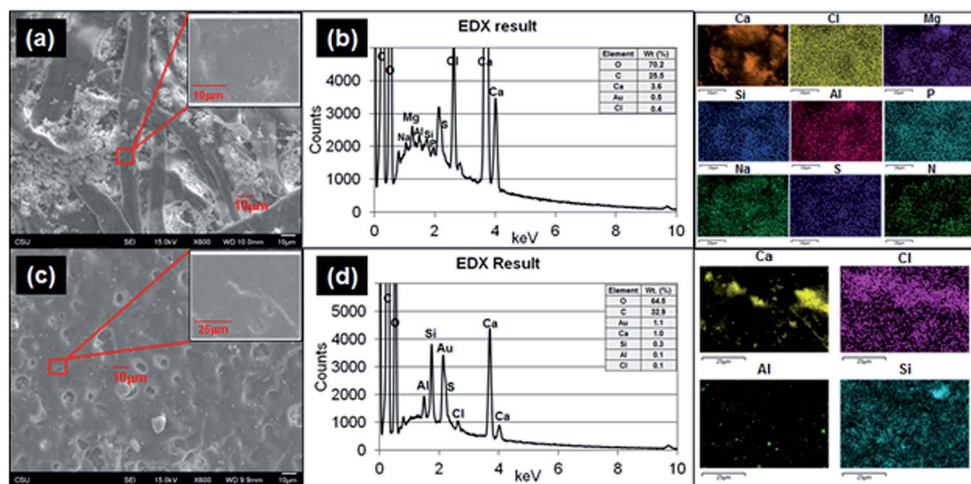


Fig. 7 Microscopy analysis of paper particles from shredding plain and printed paper. (a) SEM images of plain paper at low and high magnification. (b) EDS quantitative and qualitative analyses of image (a), plain paper. (c) SEM images of printed paper at low and high magnification. (d) EDS quantitative and qualitative analysis of image (c), printed paper. Note: Gold (Au) was used as a coating in this analysis and was excluded.

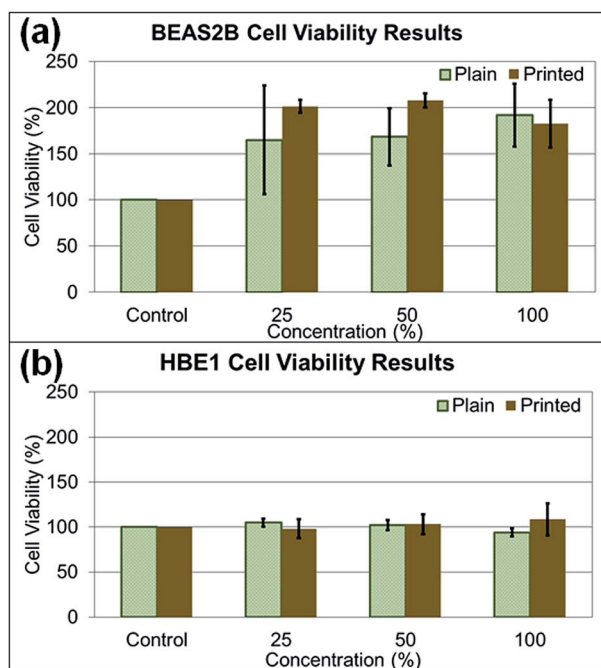


Fig. 8 Cell viabilities in two different cell lines (BEAS2B and HBE1) after paper particle exposure for 24–48 h. The mean values of each concentration are presented in bar graphs as a percentage with respect to the control in each cell line not exposed to paper particles. Error bars are standard error of the mean. (a) Changes in viability in the BEAS2B cell line. (b) Changes in viability in the HBE1 cell line.

identified from plain paper, and Ca from printed paper, on both instruments. However, the remaining elements identified from SP-ICP-MS, such as Br, Cu, Fe, and Ni from plain paper, and Br, Fe, and P from printed paper, did not overlap with the EDS results. Cl, Mg, Na, S, and Si, the other elements identified in EDS analysis, were not detected in SP-ICP-MS analysis. The elemental composition analysis of paper particles showed

limited overlapping constituents in SP-ICP-MS and EDS analysis. This discrepancy may be explained by the sample preparation process for SP-ICP-MS analysis, such as centrifuging, dilution, and removal of some paper particles to form evenly suspended solution, the variation of instrument detection limits and operating sensitivity. The EDS analyzes samples directly on particle or paper without processing any treatment or further laboratory procedures. As observed from the results, the use of different analytical instrument may alter the composition of samples due to the sample preparation procedures.

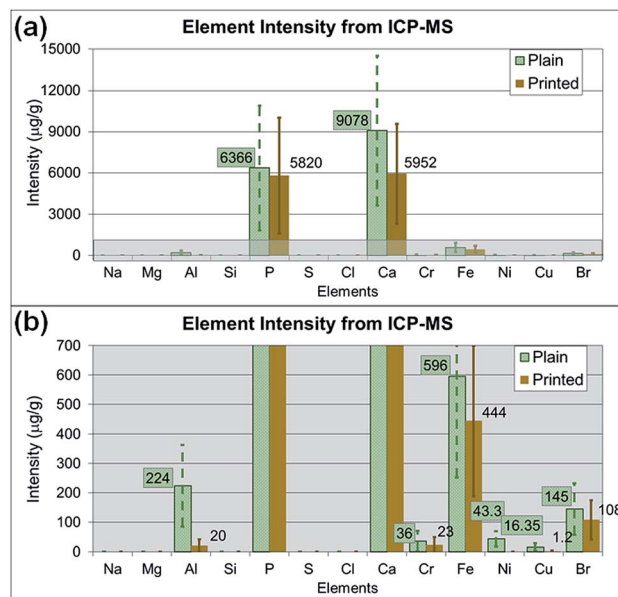


Fig. 9 Average element intensities of paper particles in media used for cytotoxicity assays, with standard error bars of each mean measured by SP-ICP-MS, representing the net intensity difference after subtraction of the blank sample. (a) Overall intensity results at a scale up to 15 000  $\mu\text{g g}^{-1}$ . (b) Intensity results at a scale less than 700  $\mu\text{g g}^{-1}$  of the highlighted area in (a).



## Conclusions

In conclusion, this study showed substantial particle release from printer printing and that those particles contained various elements. Shredding of printed paper released fewer particles than shredding of plain paper. A review article regarding indoor air qualities of PM 2.5 and PM 10 has reported the particle concentrations measured at various locations (homes, schools, offices and aged care facilities). Comparisons of the measurements using different instruments are challenging because some instruments measure particle in aerodynamic size or mobility size. Our measurements using NanoScan SMPS and OPS have shown the particle number concentrations in a range of hundreds to thousands of particles per cubic centimeters for particles less than 2.5  $\mu\text{m}$ , which represents PM 2.5. Other studies have shown the PM 2.5 measurements in the range from 1200 to  $1.2 \times 10^6$  particles per  $\text{cm}^3$  at various indoor locations.<sup>30</sup> The contribution of particles released from printer and shredder use to the indoor air in such environments<sup>30</sup> will add to the indoor particles and may become of concern, especially for susceptible people. The cytotoxicity tests on BEAS2B and HBE1 cells exposed to paper particles showed no toxicity; thus, the findings are inconclusive regarding additional potential health effects. However, the metal elements found on paper pieces and particles are known to have adverse health effects after excessive exposure; the health outcomes from such exposure may vary depending on an individual's susceptibility and health condition. Additional cellular endpoints, such as inflammatory mediators and wound healing, will need to be further evaluated in the future.

## Conflicts of interest

The authors declare no conflicts of interest.

## Acknowledgements

This research was funded by the Education and Research Center (grant #T42/OH008432-09) and Centers for Disease Control and Prevention (grant #T42/OH0092-29). The contents are solely the responsibility of the authors and do not necessarily represent the official views of the Centers for Disease Control and Prevention or the Department of Health and Human Services. The authors thank Dr Roy Geiss for technical support in TEM and EDS analysis and Dr Jacqueline Chaparro for technical analysis through SP-ICP-MS. The authors thank TSI Incorporated for their collaboration and consultation regarding instrument operation and maintenance.

## References

- 1 A. J. Koivisto, T. Hussein, R. Niemelä, T. Tuomi and K. Hämeri, Impact of particle emissions of new laser printers on modeled office room, *Atmos. Environ.*, 2010, **44**, 2140–2146.
- 2 J. Sundell, H. Levin, W. W. Nazaroff, W. S. Cain, W. J. Fisk, D. T. Grimsrud, F. Gyntelberg, Y. Li, A. K. Persily,

- A. C. Pickering, J. M. Samet, J. D. Spengler, S. T. Taylor and C. J. Weschler, Ventilation rates and health: multidisciplinary review of the scientific literature, *Indoor Air*, 2011, **21**, 191–204.
- 3 C. Paolo and W. Peder, Assessment of Indoor Air Quality Problems in Office-Like Environments: Role of Occupational Health Services, *Int. J. Environ. Res. Public Health*, 2018, **15**, 741.
- 4 E. R. Jayaratne, X. Ling, C. He and L. Morawska, Monitoring charged particle and ion emissions from a laser printer, *J. Electrostat.*, 2012, **70**, 333–338.
- 5 S. Melching-Kollmuss, W. Dekant and F. Kalberlah, Investigations on fine and ultrafine particles released from laser printers and photocopiers as indoor air contaminants in German office rooms, *N. Schmied. Arch. Pharmacol.*, 2009, **379**, 90–91.
- 6 S. Karrasch, M. Simon, B. Herbig, J. Langner, S. Seeger, A. Kronseder, S. Peters, G. Dietrich-Gumperlein, R. Schierl, D. Nowak and R. A. Jorres, Health effects of laser printer emissions: a controlled exposure study, *Indoor Air*, 2017, **27**, 753–765.
- 7 C. He, L. Morawska and L. Taplin, Particle Emission Characteristics of Office Printers, *Environ. Sci. Technol.*, 2007, **41**, 6039.
- 8 J. H. Byeon and J.-W. Kim, Particle emission from laser printers with different printing speeds, *Atmos. Environ.*, 2012, **54**, 272–276.
- 9 C. He, L. Morawska, H. Wang, R. Jayaratne, P. McGarry, G. Richard Johnson, T. Bostrom, J. Gonthier, S. Authemayou and G. Ayoko, Quantification of the relationship between fuser roller temperature and laser printer emissions, *J. Aerosol Sci.*, 2010, **41**, 523–530.
- 10 R. Bai, L. Zhang, Y. Liu, L. Meng, L. Wang, Y. Wu, W. Li, C. Ge, L. Le Guyader and C. Chen, Pulmonary responses to printer toner particles in mice after intratracheal instillation, *Toxicol. Lett.*, 2010, **199**, 288–300.
- 11 S. Pirela, I. Miousse, X. Lu, V. Castranova, T. Treye, Y. Qian, D. Bello, L. Kobzik, I. Koturbash and P. Demokritou, Effects of Laser Printer-Emitted Engineered Nanoparticles on Cytotoxicity, Chemokine Expression, Reactive Oxygen Species, DNA Methylation, and DNA Damage: A Comprehensive *in Vitro* Analysis in Human Small Airway Epithelial Cells, Macrophages, and Lymphoblasts, *Environ. Health Perspect.*, 2016, **124**, 210.
- 12 C. S.-J. Tsai, N. Shin, A. Castano, J. Khattak, A. M. Wilkerson and N. R. Lamport, A pilot study on particle emission from printer paper shredders, *Aerosol Sci. Technol.*, 2017, **51**, 57–68.
- 13 J. D. Sisler, S. V. Pirela, S. Friend, M. Farcas, D. Schwegler-Berry, A. Shvedova, V. Castranova, P. Demokritou and Y. Qian, Small airway epithelial cells exposure to printer-emitted engineered nanoparticles induces cellular effects on human microvascular endothelial cells in an alveolar-capillary co-culture model, *Nanotoxicology*, 2015, **9**(6), 769–779.
- 14 N. Kagi, Ultrafine Particle Contamination in Indoor Air and Emission from Printers, *Eurozoru Kenkyu*, 2008, **23**, 252–256.



- 15 M. Scungio, T. Vitanza, L. Stabile, G. Buonanno and L. Morawska, Characterization of particle emission from laser printers, *Sci. Total Environ.*, 2017, **586**, 623–630.
- 16 Z.-M. Wang, J. Wagner and S. Wall, Characterization of Laser Printer Nanoparticle and VOC Emissions, Formation Mechanisms, and Strategies to Reduce Airborne Exposures, *Aerosol Sci. Technol.*, 2011, **45**, 1060–1068.
- 17 M. Wensing, T. Salthammer, C. He, L. Morawska, T. Schripp and E. Uhde, Evaluation of Ultrafine Particle Emissions from Laser Printers Using Emission Test Chambers, *Environ. Sci. Technol.*, 2008, **42**, 4338–4343.
- 18 C. Tsai and D. Theisen, A sampler designed for nanoparticles and respirable particles with direct analysis feature, *J. Nanopart. Res.*, 2018, **20**, 1–14.
- 19 R. Reddel Roger, K. Yang, R. Johng, E. Brash Douglas, R. Su, F. Lechner John, I. Gerwin Brenda, C. Harris Curtis, A. Paul Camperdown and Australia assigned to The United States of America as represented by the Department of Health and Human Services, 5443954 Immortalized non-tumorigenic human bronchial epithelial cell lines, *Biotechnol. Adv.*, 1996, **14**, 514.
- 20 J. Lechner and M. LaVeck, A serum-free method for culturing normal human bronchial epithelial cells at clonal density, *J. Tissue Cult. Methods*, 1985, **9**, 43–48.
- 21 O. Sakamoto, A. Iwama, R. Amitani, T. Takehara, N. Yamaguchi, T. Yamamoto, K. Masuyama, T. Yamanaka, M. Ando and T. Suda, Role of macrophage-stimulating protein and its receptor, RON tyrosine kinase, in ciliary motility, *J. Clin. Invest.*, 1997, **99**, 701.
- 22 R. J. Hay, J. Caputo and M. Macy, *ATCC quality control methods for cell lines*, Amer Type Culture Collection, 1992.
- 23 J. Caputo, Biosafety procedures in cell culture, *J. Tissue Cult. Methods*, 1988, **11**, 223–227.
- 24 D. O. Fleming, J. H. Richardson, J. J. Tulis and D. Vesley, *Laboratory safety: principles and practices*, ASM Press Washington, DC, 1995.
- 25 J. R. Yankaskas, J. E. Haizlip, M. Conrad, D. Koval, E. Lazarowski, A. M. Paradiso, C. A. Rinehart, B. Sarkadi, R. Schlegel and R. C. Boucher, Papilloma virus immortalized tracheal epithelial cells retain a well-differentiated phenotype, *Am. J. Physiol.: Cell Physiol.*, 1993, **264**, C1219–C1230.
- 26 A. B. Alexander, Thermal properties of graphene and nanostructured carbon materials, *Nat. Mater.*, 2011, **10**, 569.
- 27 C. Monn, A. Fuchs, D. Högger, M. Junker, D. Kogelschatz, N. Roth and H. U. Wanner, Particulate matter less than 10  $\mu\text{m}$  (PM 10) and fine particles less than 2.5  $\mu\text{m}$  (PM 2.5): relationships between indoor, outdoor and personal concentrations, *Sci. Total Environ.*, 1997, **208**, 15–21.
- 28 T. Osunsanya, G. Prescott and A. Seaton, Acute respiratory effects of particles: mass or number?, *Occup. Environ. Med.*, 2001, **58**, 154.
- 29 R. S. Osgood, B. L. Upham, P. R. Bushel, K. Velmurugan, K.-N. Xiong and A. K. Bauer, Secondhand Smoke-Prevalent Polycyclic Aromatic Hydrocarbon Binary Mixture-Induced Specific Mitogenic and Pro-inflammatory Cell Signaling Events in Lung Epithelial Cells, *Toxicol. Sci.*, 2017, **157**, 156–171.
- 30 L. Morawska, G. A. Ayoko, G. N. Bae, G. Buonanno, C. Y. H. Chao, S. Clifford, S. C. Fu, O. HäNninen, C. He, C. Isaxon, M. Mazaheri, T. Salthammer, M. S. Waring and A. Wierzbicka, Airborne particles in indoor environment of homes, schools, offices and aged care facilities: The main routes of exposure, *Environ. Int.*, 2017, **108**, 75–83.

